Evaluation of Developmental Toxicity and Oxidative Stress Caused by Zinc Oxide Nanoparticles in Zebra fish Embryos/ Larvae

Deenathayalan Uvarajan
PSG College of Arts and Science
Nandita Ravichandran
Bharathiar University
Kavithaa Krishnamoorthy
Hindustan Arts & Science College
Kavithaa Vengamuthu Subramaniyan
Vellalar College for Women
Govindasamy Chandramohan
King Saud University College of Applied Medical Sciences
Al-Numair Khalid S.
King Saud University College of Applied Medical Sciences
Alsaif Mohammed A.
King Saud University College of Applied Medical Sciences
Cheon Yong Pil
Sungshin Women's University
Arul Narayanasamy
Bharathiar University
Brindha Durairaj (publicationbiochemistry@gmail.com)
PSG College of Arts and Science

Research Article

Keywords: Zinc oxide nanoparticles, zinc accumulation, Teratogenicity, Nanotoxicity, zebrafish embryotoxicity test (ZET)

Posted Date: October 13th, 2023

DOI: https://doi.org/10.21203/rs.3.rs-3061912/v1

Version of Record: A version of this preprint was published at Applied Biochemistry and Biotechnology on November 21st, 2023. See the published version at https://doi.org/10.1007/s12010-023-04791-5.

Abstract

Zinc oxide nanoparticles (ZnO NPs) are used in various fields, including biological ones. ZnO NPs are eventually disposed of in the environment where they may affect natural systems, and there is no international law to regulate their manufacture, usage, and disposal. Hence, this present study is carried out to synthesize a more non-toxic and bioactive ZnO NPs from the marine algae *Sargassum polycystum*. The ZnO NPs were biologically produced using the marine algae *Sargassum polycystum*. The Dynamic light scattering result describes that synthesized particles average size about 100nm in diameter Transmission electron microscopy (TEM) analysis demonstrated the rod like morphology of ZnO NPs. Fourier transmission infrared spectroscopy (FT-IR) results revealed the presence of functional groups in ZnO NPs. The selected area electron diffraction (SAED) results strongly suggested the ZnO NPs crystallinity. ZnO NPs surface morphology and compositions were identified by scanning electron microscopy (SEM- EDX) values. To analyse the toxicity of synthesized nanoparticles zebra fish larvae were used, which involved subjecting embryos to various ZnO NPs concentrations at 1 hpf and analysing the results at 96 hpf. The 60 and 80 ppm sub-lethal doses were chosen for further studies based on the LC_{50} (82.23 ppm). In the ZnO NPs treated groups, a significant slowdown in pulse rate and a delay in hatching were seen, both of which impacted the embryonic processes. A teratogenic study revealed a dose-dependent increase in the incidence of developmental deformities in the treated groups. Along with increased oxidants and a corresponding reduction in antioxidant enzymes, Na^+ K^{+-}ATPase and AChE activity changes were seen in ZnO NPs treated zebra fish larvae groups. The apoptosis process was increased in ZnO NPs treated groups revealed by acridine orange staining. These results indicate that the green synthesis process cannot mitigate the oxidative stress induced by ZnO NPs on oxidative signalling.

Introduction

Several sectors benefit from marine science research and innovation, including pharmaceuticals, environmental trends, nanomedicine, and food. Around 25,000 biologically active compounds with various applications are present in the marine ecosystem. Marine fungi, bacteria, and seaweed could all be used to fight against infectious diseases [1]. Prior studies indicate that the marine-derived chemicals market has topped USD 10 billion [2]. There has been a lot of interest in developing marine-based nanoparticles from various sources, such as bacteria, fungi, seaweeds, and marine plants for biomedical applications. Much attention has recently been paid to nanomaterials ecotoxicity. ZnO NPs are a growing global concern due to their wide variety of uses and applications. Since 1935, scientists have paid much attention to ZnO NPs because they are potentially a useful future material [3]. Applications in nano diagnostics, nanomedicine, and antimicrobials extensively used ZnO NPs [4].

Seaweeds are mainly employed for industrial purposes but are not yet widely imposed for nanoparticle biosynthesis worldwide. Less research has been done on the antibacterial and antifungal [5] properties of ZnO NPs made by seaweed. ZnO NPs with improved bioactivity can be made by combining them with marine algal extracts. Therefore, ZnO NPs derived from marine algae have the potential to display enhanced biological activities. *S. polycystum* belongs to the *Chromista* kingdom and *Ocrophyta* phylum.

Marine brown algae (Phaeophyta) *Sargassum* are classified in a higher order called the *Fucales* and *Saragassaceae* family. It has been reported that the antioxidant and free radical scavenging properties of *S. polycystum* helped to reduce the hyperglycaemia and dyslipidaemia in diabetic rats [6]. Previous reports suggest that *S. polycystum* is an effective agent against psoriasis and is used to treat ulcers and lung diseases [7]. NPs can produce toxic metabolites, which are responsible for the stress on organisms. Several techniques can be used to investigate the cytotoxic effects of a chemical on living tissue and cells.

A well-established model for studying NPs-induced developmental toxicity is the zebrafish (*Danio rerio*) [8]. Zebrafish and humans have a high degree of genomic similarity, making it simple to extrapolate the teratogenic effects from zebrafish to humans [9]. In several models, including the zebrafish, the developmental toxicity caused by ZnO NPs has been investigated [10]. The impact of NPs on redox homeostasis is made more accessible by changes in the oxidant and antioxidant indicators. A cholinergic enzyme, acetylcholinesterase (AChE), along with $Na^{+}K^{+}$-ATPase has also been used as a toxicological marker for foreign substances that regulate osmoregulation [11]. These biomolecules can be exploited as efficient NPs toxicity warning systems. This research was conducted in zebra fish embryos and larvae to achieve the following aims: (i) To determine the concentration of *S. polycystum* NPs associated with teratogenicity; (ii) To investigate developmental defects brought on by ZnONPs exposures below lethal levels, and (iii) To investigate the impact of oxidative stress caused by ZnO NPs on teratogenicity. However, no studies have been centred on the effect of *S. polycystum* mediated ZnO NPs. Hence, this research was carried out to identify the toxicity and biocompatibility of ZnO NPs obtained from *S. polycystum.*

Materials and Methods

Chemicals

Zinc sulphate heptahydrate was procured from Sigma Aldrich. All additional compounds were of the analytical grade. The E3 medium and the solutions for the biochemical analyses were made with double-distilled water.

Collection and identification of Seaweeds

Seaweeds were collected in the shallow waters of the Gulf of Mannar, Mandapam on India's southeast coast. Algae were identified using morpho-taxonomic characteristics and the taxonomic monographs of Trono (1997) and Algae Base [12]. The collected seaweeds were washed in tap water to remove all the debris before being rinsed for around 15 minutes in distilled water. After being air-dried, the seaweeds were chopped into little pieces, ground into powder, and used for more research.

Preparation of seaweed extract

10g of seaweed powder and 100 ml of water were mixed to create the seaweed algal extract. Following a 24-hour period of constant shaking, the mixture underwent filtering, and the solvent was gathered [13].

Biosynthesis of ZnO NPs from aqueous extract of S. polycystum

300 ml of aqueous zinc sulphate heptahydrate (4 mM) and 10 ml of the aqueous extract were combined and agitated at room temperature for 5 minutes until the solution turned pale yellow. Then, 1M sodium hydroxide solution was added to the mixture while stirring at room temperature. The particles were made clean by mixing the suspended particles with sterile distilled water. To clean up the final product's contaminants, ethanol was used to wash the white particles that had been obtained. The white powder was vacuum-dried for six hours at 60^{o}C, and the sample was kept for further experiments [14].

Dynamic light scattering analysis (DLS)

A particle size analyser was used to verify the size distribution and polydispersity index (PI) of the synthesised ZnO NPs. To examine NPs' colloidal dispersion, a Horiba analyser (SZ-100) was used. At 25^{o}C and a scattering angle of 90 degrees, dynamic light scattering (DLS) is used to determine the particle size [15].

Scanning electron microscopy (SEM) and EDX analysis

SEM analysis of ZnO NPs under dry conditions was used to determine their shape and average size distribution. After being dried, ZnO NPs were stationed at a conducting, customised copper grid for SEM analysis by Hassellöv et al. techniques [16]. An energy-dispersive X-ray system (EDX) examination was performed to confirm the elements that comprise the ZnO NPs.

Transmission electron microscopy (TEM) analysis

The experiment used a Tecnai G2 20 (FEI) S- Twin electron microscope with a 20 kV accelerating voltage. By placing a spot of colloid solution on a copper screen with a mesh size of 400 nm covered in an amorphous carbon film and letting the solvent evaporate in room temperature air, specimens for TEM measurement were produced [17].

Selected area electron diffraction (SAED) analysis

The SAED pattern is used to verify the texture and crystallinity of synthesised nanoparticles, making it an essential tool in the field of nanomaterial sciences. It can be modified to extract specific information from the synthesized nanoparticles, serving as a characterization tool for better comprehending the diffraction pattern of a targeted region [15].

Fourier transforms infrared spectroscopy (FT- IR) analysis

Using a KBr pellet and FT-IR (M/S JASCO, U.S.A.) in the transmittance mode, the functional group of the materials is verified. A microscope that is attached to the main instrument allows for the examination of limited sample sizes. A microscope attached to the primary device provides for the analysis of small

sample areas. *S. polycystum* mediated ZnONPs were analysed by placing the powder under a microscope and shifting the laser photons' energies up or down. The energy change details the system's vibrational modes [18].

Thermogravimetric (TGA) analysis

TGA analysis was used to determine the thermal stability of ZnO nanoparticles synthesized from *S. polycystum*. A TGA- DTA analyser (Perkin Elmer, STA 6000, USA) was used to analyse the thermal properties of synthesized nanoparticles. The temperature was raised from 40- 730^{o}C at a rate of 10^{o}C min^{-1}[19].

Zebra Fish maintenance and embryo collection

A commercial breeding facility was used to obtain adult zebrafish (Chennai, India). In the aquatic facility, fishes were kept at 28°C with a photoperiod of 10 hours of darkness and 14 hours of light. Commercially available freeze-dried blood worms were given to them three times daily for food. Male and female fish were kept together in a separate glass tank for spawning 12 hours before dawn in a 2:1 ratio to obtain embryos. Using nylon mesh that was the right size so that the embryos could sink to the bottom of the aquarium tank helped reduce egg predation by the fish. Being photoperiodic breeders, zebra fish spawn about 20 to 30 minutes before sunrise. After shifting the water via the filter, the embryos were then collected. The unfertilised eggs were taken out after they were examined using an inverted fluorescent microscope (Optika IM 3). The fertilised embryos were staged and used in all of the tests by Kimmel et al. [20]. The exposure medium, known as E3 medium (0.17 mM KCl, 5 mM NaCl,0.33 mM $MgSO_4$ and 0.33 mM $CaCl_2$ with pH 6.9–7.1), was used to preserve the embryos. All the experimental protocols adhered fully to the rules established by the PSG College of Arts & Science's ethical committee for using experimental animals.

Zebra fish embryos to NPs exposure

The embryo test process was the foundation for the acute toxicity assay [21]. Freshly made stock ZnO NPs (200 ppm) were ultrasonically processed for 30 min (40 kHz, 50 W) utilising the ultrasonic processor. In a 24-well multi-plate with one embryo per well, the embryos were exposed to ZnO NPs at various concentrations (0- 140 ppm) in a 2 ml medium. Starting at 1hourpost-fertilisation (hpf), the exposure was static and continued nonstop for 96 hpf. Throughout the whole exposure period, the ZnO NPs suspensions were not replenished. All 24-well multi-plates containing embryos were kept at 28°C with a 14hour and10hour dark cycle. If there is no heartbeat, the larvae are assumed to be dead. When the exposure is over (96 hpf), the LC_{50} was determined using Finney's probit analysis approach [22].

Phenotypic changes in developing zebrafish embryo

The exposure time ranged from 1 to 96 hpf, and the groups include control, 60, and 80 ppm. When a larva's entire body was expelled from the chorion, it was deemed to have hatched. Depending on how many larvae are fertilized and developed into viable embryos, the overall hatching success rate was calculated in percentage [23]. A 96 hpf observation of teratogenicity was made. Teratogenicity comprises

body differentiation, heartbeat, gross deadly lesion, lesion of the embryo, and death. The embryo's pulse rate was measured by manually counting the beats that occurred at 10-second intervals and converting those counts into beats per minute (bpm). Specific endpoints were chosen based on the potential for straightforward measurement and management. Developmental milestones in control and ZnO NPs-treated embryos were examined by an inverted fluorescent microscope with a digital camera. The morphological study was reproduced with 10 larvae in each group with triplicates. Zebra fish larvae were killed by being immersed in ice water for 20 minutes before being utilised for further study [21].

Na^+ K^+ ATPase, AChE activity and total protein content

In the ice-cold phosphate buffer, the treated and control larvae were homogenized after the exposure period. The supernatant was used for additional biochemical testing following the centrifugation of homogenates at 14,500xg at 4^oC for 15 minutes. Quantification of the total protein content was done using the Lowry et al. technique [24]. Using 5 ml of alkaline copper reagent, 0.1 ml of recovered homogenate was diluted to 1 ml using distilled water. It was thoroughly mixed and allowed to incubate for ten minutes at 37°C. After the initial incubation, 0.5 ml of 1 N Folin-Ciocalteu phenol reagent was added. As a standard, bovine serum albumin (BSA) was used. The intensity of the blue colour was measured at 620 nm. The amount of protein is expressed as mg/g.

The Ellman et al. technique was used to measure the AChE activity [25]. The experiment was initiated by mixing 50 µl of homogenate with a composition of reaction mixtures, including 100 µl of 10 mM 5,5'-dithiobis and 50 µl of 1 M potassium phosphate buffer. Then, the 20 µl of 25 mM acetylthiocholine iodide was added and incubated for 10 min at 37°C. The development of a yellow colour was read at 412 nm. AChE activity is measured in units (U) per mg of protein.

The Na + K+-ATPase activity was measured using the bonting technique [26]. Once the reaction mixture has been incubated at 37°C for 10 minutes, additional ingredients are added, including 50 mM $MgSO_4$, 50 mM KCl, 60 mM NaCl, 4 mM ATP, Tris buffer, and 1 mM EDTA. 0.1 ml of homogenate was added to this mixture, and it was then incubated at 37°C for 15 minutes. Using the Fiske and Subbarow approach, the amount of phosphorus in the supernatant was calculated and expressed as M/min/mg [27].

Antioxidant and oxidative markers

The Beauchamp and Fridovich technique was used to quantify the reactive oxygen species (ROS) produced [28]. For each group 30 larvae were homogenised in 1 ml of Hank's balanced salt solution (HBSS). The mixture of this solution was incubated for 8 hours at 37°C. After centrifugation for 10 min at 14000xg, the resulting pellets were rinsed three times with methanol. The samples were dispersed in 1 ml of DMSO and 2 M KOH. Absorbance at 630 nm was used to quantify ROS formation as a percentage.

Using the approach developed by Devasagayam and Tarachand [29], lipid peroxidation (LPO) was evaluated. The reaction mixture contains 0.15 ml of 10 mM KH_2PO_4, and 0.5 ml of 0.15 M Tris-HCl buffer (pH 7.4), received 0.1 ml of the sample. The mixture was incubated for 20 minutes at 37°C while

vigorously shaken.10% TCA was added to halt the reaction. The resulting MDA was detected at 532 nm, and the concentrations are given in nM/mg.

Levine et al. approach calculated the amount of protein carbonyl [30]. The homogenate was added to the test and control tubes at a volume of 1.0 ml. The test tube received 2.5 M HCl (4.0 ml) and 4.0 ml of 10 mM DNPH, while the control received 2.5 M HCl alone. The tubes were vortex and then kept at 37^{o}C for 1hourin the dark. The process was halted by adding 5 ml of 20% TCA to the control and treated tubes. The protein pellet was recovered after 15 minutes of centrifugation at 14000xg. The shot was further rinsed with ethanol and TCA (1:1). The pellet was treated with 2 ml of 6 M guanidine hydrochloride and then incubated for 10 minutes at 37°C. The PC concentration was determined at 490 nm and expressed as nM/mg.

Nitric oxide (NO) levels in the treatment and control groups were determined by applying the Green et al. approach [31]. A 0.25 ml homogenate was used to dilute the Griess reagent, which was then incubated for 15 minutes at 37°C. The absorbance at 546 nm was calculated and expressed as µM/mg. To ascertain the effect of ZnO NPs on antioxidant enzymes, tests were conducted on the key antioxidant enzymes catalase (CAT), glutathione peroxidase (GPx), superoxide dismutase (SOD), and glutathione S transferase (GST). The applied technique was slightly modified according to Thirumurthi et al. to calculate the SOD activity in zebra fish larvae head [21]. Ice-cold ethanol (0.25 ml) and chloroform (0.15 ml) were combined with 0.5 ml of homogenate and maintained in a shaker for 15 minutes. The supernatant (0.5 ml) from the centrifugation of the mixture at 14,500xg for 15 minutes was utilised for further analysis. Tris-HCl buffer (2 ml, pH 8.2), 2 mM pyrogallol (0.5 ml), and 2.0 ml of distilled water were added to the supernatant. Pyrogallol auto oxidation was measured at 430 nm once per minute for three minutes, regarded as the autooxidation rate (100%). A final volume of 4.5 ml was made by combining 0.5 ml of 2 mM pyrogallol, Tris-HCl buffer (2 ml, pH 8.2), 0.5 ml aliquots of the enzyme and 1 ml of distilled water. 2.5 ml of distilled water and 2.0 ml of Tris-HCl buffer (pH 8.2) were combined as a blank. The enzyme activity was expressed as U/mg protein. The Aebi technique was used to assess the amount of the CAT enzyme [32]. 0.5 ml of H_2O_2 and 1 ml of phosphate buffer were added to 1 ml of homogenate. The reaction was stopped by adding 2 ml of dichromate acetic acid at various intervals (0–60 s). The activity was quantified as U/mg protein and measured at 590 nm.

The Rotruck technique was used to evaluate GPx activity as previously reported [33]. The glutathione S-transferase (GST) levels were determined according to a method developed by Habig and Jakoby [34]. 150 µL of 1-chloro-2, 4-dinitrobenzene (CDNB), 150 µL of sample, and 50 µL of 25 mM GSH make up the reaction mixture. Three minutes later, the absorbance was measured at 340 nm. The unit of measurement for the particular enzyme activity was U/mg protein.

Acridine orange(AO) staining

The amount of apoptosis brought on by the ZnO NPs was determined by AO staining [35]. The treated and control larvae were washed twice in ice-cold PBS. Zebra fish larvae were stained with AO (5 µg/ml) and incubated in a dark room for 1 hour. The larvae were then repeatedly rinsed with distilled water before

the inspection. With an Optika IM 3 inverted fluorescent microscope and a blue filter, apoptotic cells were identified [21].

Statistical analysis

All experiments were performed with at least three replicates and the mean± SD was used to express the findings. The assumptions were satisfied, and one-way analysis of variance (ANOVA) was used to compare the control and ZnO NPs treatment groups. Studies with a p-value of 0.05, 0.01 and 0.001 were statistically significant. The statistical analysis was done by using GraphPad Prism 9.0.

Results and Discussion

Our work evaluated the physicochemical properties of the synthesised ZnO NPs and their teratogenic potential, oxidative stress, and mortality in zebra fish embryos. A thorough explanation of the physicochemical properties is necessary to comprehend how these ZnO NPs affect toxicological classification [36]. Our previous studies reported the UV- vis spectrum, zeta potential, and XRD pattern of *S. polycystum-mediated* ZnO NPs [37]. Furthermore, to identify the toxicity mechanism of these ZnO NPs, an extensive study was carried out in zebrafish larvae. Our SEM study showed the surface morphology of *S. polycystum-mediated* ZnO NPs (sup Fig. 1a). In SEM pictures, ZnO NPs were discovered to be rod-shaped and had an estimated size ranging from 32 to 34 nm. The EDX pattern of ZnO NPs revealed no contaminants were present in it (sup Fig. 1b). ZnO NPs TEM images are displayed in (sup Fig. 1c).To comprehend the crystalline properties and size of the nanoparticles, a TEM examination was conducted. The TEM images of ZnO NPs corroborate the SEM findings that the particles are almost hexagonal with slight thickness variations. In SAED pattern, specific areas of TEM image are displayed as diffraction spots to view and quantify their crystalline properties. The SAED analysis used to determine whether the particle is amorphous, polycrystalline, or single-crystalline. SAED pattern of ZnO NPs were shown in (Sup Fig. 1d). On the image, bright spots were seen along with a concentric ring pattern. It is further demonstrated that the synthesized particles have a crystalline structure.

DLS analysis revealed that the synthesised ZnO NPs come in a wide range of sizes. Distribution of particle sizes was found to be range between 6 nm and 195 nm, but average particles size was measured about 100 nm (Fig. 1a). Smaller NPs are often more hazardous than their bigger equivalents. In order to assess the ZnO NPs purity and thermal stability, TGA analysis was performed. TGA results of ZnO NPs from *S. polycystum* (Fig. 1b) revealed multiple decompositions and weight loss, possibly due to chemical bond breaks or interactions with secondary metabolites. Decomposition of the ZnO NPs is primarily caused by the core material, nitrogen, and oxygen. TGA analysis of *S. polycystum* mediated ZnO NPs showed good thermal stability up to 600^{o}C. The FTIR spectra of ZnO NPs obtained between 400 and 4000 cm^{-1}are displayed in Fig. 2. The solitary bridge of O-H stretching was represented by a broad peak in the FTIR spectrum at 3094 cm^{-1}. The absorption of C = O by metallic cations in the ZnO NPs may account for the peak at 1743 cm^{-1}. The integration of ZnO NPs into functional bio-molecules was

verified with the FT-IR spectrum. The observations of Sakthivel et al. who synthesised ZnO NPs from *Citrus limon*, are highly correlated with all the above characterization results [38].

Effects of ZnO NPs on hatching, lethality and heart beat rate

In this research, overexposure of ZnO NPs led to lethality in a dose-dependent manner (Fig. 2). The LC_{50} value for embryos was determined using probit analysis to be 82.23 ppm for 96 hpf. The lower and upper confident levels are mentioned in (sup. table 1.) The sub-lethal dose of 60 and 80 ppm was selected for further studies based on LC_{50}. The doses were used to explore the effects of *S. polycystum-mediated* ZnO NPs on zebra fish embryos and larvae at sub-lethal levels. ZnO NPs colloidal instability causes them to precipitate at the base frequently. This precipitate is brought on by the NP's decreased reactivity and dispensability. As a result, ZnO NPs have more time to interact with the embryos before they hatch. Additionally, the ZnO NPs aggregation may obstruct the chorion membrane pore channels and reduce oxygenation. In accordance with a previous report, this finding indicates that zebrafish larvae are more vulnerable to ZnO NPs at higher mass concentrations [39].

Hatching is a critical sign of toxicity since it is a complex biological process that is impacted by a number of factors. The rate at which the control, 60, and 80 ppm ZnO NPs treated groups hatched was measured at three separate time points between 48 and 96 hpf (Fig. 3a). Due to a time and dose-dependent the hatching was delayed at 96 hpf as well as exposure to ZnO NPs decreased the hatching rate by 25% at 60 ppm and 76% at 80 ppm. Contrary to earlier research by de Oliveira et al. who found no appreciable change in the hatching pace in a lower dose [40]. The embryo is surrounded by a chorion, an extraembryonic layer, which shields it from outside influences until it hatches. It has three layers: an outer layer of 0.2–0.3 m electron-dense, a middle layer of 0.3–0.6 m electron-translucent, and an interior layer of 1.0–1.6 m thick. Between the syncytial layer and vitelline membrane, it has pores that are 0.5–0.7 m in diameter and have a characteristic cone shape [41]. Smaller NPs have been shown to cause embryonic toxicity by passively diffusing via the chorionic pore canals. Additionally, it has been demonstrated that NPs can clump together in the chorion, increasing chorionic thickness [42] and obstructing the transfer of oxygen and nutrients, causing hypoxia that is harmful to growth.

In our investigation, ZnO NPs treatment groups were more likely to have bradycardia (a reduction in heart rate) than control groups in a concentration-dependent way. When 60 and 80 ppm were compared to the control, the pulse rate decreased by 15% and 26% (Fig. 3b) [43], respectively. Our results demonstrate that ZnO NPs can cause cardiac dysfunction, which may result in disorders related to the cardiovascular system. Cardiomyocyte function is altered by oxidative stress, and fluctuations in healthy cell homeostasis can result in vascular and heart diseases. In addition to oxidative stress, electrolyte imbalance caused by Na^+/K^+-ATPase has also been demonstrated to affect heart rhythm, resulting in bradycardia in zebrafish [44].

Teratogenicity

Testing for developmental abnormalities and teratogenicity are the most important approaches for assessing nanoparticle-induced toxicity. The current work looked at the prevalence of developmental anomalies throughout the time exposed in both the control and treatment groups. Growth retardation, head, sacculi/otolith, heart, end tail, rachischisis, and tail malformations are among the abnormalities in the non-axial group (Fig. 4b). In contrast scoliosis, spinal cord and end tail malformations are in the axial group (Fig. 4a). However, the control group exhibited low percentages of non-axial and axial malformation presence, but 60 and 80 ppm ZnO NPs treated groups indicated teratogenicity elevation (17% and 29%, respectively) in comparison to the control (Fig. 4c). *S. polycystum-mediated* ZnO NPs have increased malformations in accordance with the claim Bai et al. [45]. According to this research, ZnO NPs can be teratogenic through the production of ROS, inflammation brought on by oxidative stress, altered gene expression, and activation of the NF-κB, p38, MAPK, Nrf2 and various apoptotic signalling pathways. Subramanian et al. also found that ZnO NPs derived from *Syzygium cumini* were toxic to the zebra fish larvae [46].

Biochemical markers

Na^+ K^+- ATPase, AChE activity and total protein content in the zebrafish larvae were estimated. Compared to the control, there was a dose-dependent increase in the total protein concentration at 40 and 60 ppm (Fig. 5a). AChE is a significant indicator of neurotoxicity in development and cholinergic neurotransmission. Acetate and choline are produced by the hydrolysis of the vital neurotransmitter acetylcholine [47]. Acetylcholine levels raise when AChE activity declines, and this increase in acetylcholine causes cholinergic receptors to be over stimulated. Changes in neuronal and muscle functioning might result from this. In groups exposed to 60 and 80 ppm of ZnO NPs, a significant decrease in AChE activity was found (Fig. 5b). Additionally, zebra fish larvae treated with zinc oxide in a prior work demonstrated comparable outcomes, raising the possibility that NPs of transition metal oxides may exhibit a similar lethal mechanism [45]. The plasma membrane's Na^+ K^+-ATPase is an active transporter pump crucial for osmoregulation, and a sign of harmful osmoregulatory effects is present. The Na^+ K^+-ATPase activity significantly decreased in the 60 and 80 ppm groups in proportion to concentration (Fig. 5c). These findings support Suganya et al. [48] findings that decreased Na^+ K^+-ATPase activity may have caused cardiovascular dysfunction by reducing heart rate.

Oxidants and Antioxidants

The phrase "oxidative stress" refers to the disruption of redox equilibrium brought on by an unbalanced concentration of oxidants and antioxidants. Oxidative stress is a major contributor of NPs toxicity. Oxidative stress indicators were evaluated in both the treatment and control groups. There were dose-dependent variations in antioxidant and oxidant levels in the treatment groups as compared to the control groups. Oxidative stress was evidenced by a considerable dose-dependent increase in ROS, LPO, PC content, and NO following exposure to ZnO NPs (Fig. 6a–d). Superoxide anion, a notable species of ROS, was evaluated to gauge a rise in ROS. Since proteins and membrane lipids are highly reactive with ROS, it

results in tissue damage. The higher LPO concentration proved this ROS have been found to accelerate the polyunsaturated fatty acids oxidation. It has been demonstrated that LPO products can cause cell death by activating both internal and extrinsic signalling pathways [49]. One of the critical indicators for oxidative stress is PC content, which is used to identify protein oxidation. Before the decline in ATP concentration and ensuing cell death, protein oxidation occurs extremely in response to oxidative stress. Additionally, it has been demonstrated that NPs cause oxidative stress by oxidising proteins that have been adsorbed to their surface, creating a structure resembling a corona [50]. NO is a transcellular messenger that is diffuse, versatile, and pivotal in different developmental progression [51]. Enhanced NO generation has been linked to cytotoxicity, which stimulates cell apoptosis. Additionally, peroxynitrite ($ONOO^-$), a reactive nitrogen species, is created when superoxide reacts with NO. The induction of NO by iron oxide NPs has been demonstrated, consistent with our findings [52].

It has been demonstrated that teleost fish, like zebra fish, contain a variety of active defensive mechanisms to reduce the toxicity caused by xenobiotics like NPs. In treated and control larvae, the antioxidant indicators were assessed. Antioxidant enzymes, including CAT, GPx, GST and SOD, were shown to significantly decrease dose-dependently (Fig. 7a- d). These enzymes are the first line of defence in the antioxidant defence system and guard cells against damage brought on by oxidative stress. Superoxide is converted to H_2O_2 by SOD, water and oxygen by CAT. GSH, GPx and GST enzymes aid the biological reductants glutathione in converting hydrogen peroxide to oxygen and water. Various metal oxide NPs have shown a comparable reduction in the antioxidant enzymes [53]. These findings demonstrate how a reduction in antioxidants affects redox homoeostasis. Similar results by Thirumurthi et al. who found that maghemite nanoparticles decreased antioxidant enzyme activity and may have contributed to elevated oxidative stress, are consistent with these findings [28].

Acridine Orange (AO) staining

Apoptosis may be sparked by an increase in oxidants. The construction of many organs and structures during embryonic development is greatly aided by apoptosis. Apoptosis is commonly described in NPs and their bulk equivalents; nevertheless, dysregulated apoptosis caused teratogenicity by xenobiotic leads [54]. By using AO staining, the apoptotic cell death in treated and control larvae was revealed (sub Fig. 3). During the early development of zebra fish embryos, apoptosis plays a vital role [55]. For this reason, you may notice some apoptotic bodies on the caudal fins of the control group. The markings were more noticeable near the tail. However, in the 60 and 80 ppm treated larvae had a significant occurrence of green patches, suggesting a higher rate of apoptosis. It has been demonstrated that uncoated ZnO NPs may cause apoptosis [56, 57]. These findings support the hypothesis that oxidative stress caused by ZnO NPs results in NPs-induced apoptosis. Validation is still required for the spatial localisation and the altered signalling pathways leading to apoptosis.

Conclusion

The aqueous extract of *S. polycystum* was used in this study to create ZnO NPs using an easy, environmentally friendly green synthesis approach. The reaction mixture's colour change served as the first indicator of ZnO NPs formation. An FTIR spectrum was used to determine the biomolecules responsible for the reduction, capping, and stability of ZnO NPs. Bio-reduced ZnO NPs with an average size of roughly 100 nm were examined for morphology using HR-TEM. EDX examination revealed that the produced ZnO NPs included numerous additional components in addition to 22.94% Zn. The findings of this study indicate the notable thermal stability of ZnO NPs produced via biosynthesis from marine algae. These study conclusions include the following: neurotoxicity, decreased rates of hatching and survival, and developmental abnormalities in zebra fish larvae exposed to 80 ppm of ZnO NPs. Based on the findings, *S. Polycystum* ZnO NPs may be hazardous because of their surface coatings, particle size, and potential for mitochondrial-DNA damage from oxidative stress. Improved comprehension of the various types of cell death processes brought on by *Sargassum polycystum* ZnO NPs will be facilitated by additional molecular study. Through the use of various marine algae supplements, we hope to reduce the toxicity of ZnO NPs on species.

Declarations

Ethics Approval

As per CPCSEA (Ministry of Fisheries, Government of India) guidelines, no *ethical approval is required for conducting research on Zebrafish (120 hpf).*

Consent to participate

Not applicable.

Consent to publish

Not applicable.

Author Contributions

All authors contributed to the study's conception and design. Arul Narayanasamy and Brindha Durairaj gave the initial ideology of the study. Deenathayalan Uvarajan and Nandita Ravichandran performed material preparation and biochemical and Staining assays. Nanoparticle characterization and analysis were done by Kavithaa Krishnamoorthy,Govindasamy Chandramohan, Al-NumairS. Khalid, and Alsaif A. Mohammed. Yong Pil Cheon performed all the Statistical analysis. Deenathayalan Uvarajan and Nandita Ravichandran wrote the initial manuscript draft and overviewed by Kavithaa Krishnamoorthy. S. Kavithaa done revision, proof reading and characterization of nanomaterial that asked by the reviewer. *All authors commented on previous versions of the manuscript. The final manuscript was read and approved by all authors.*

Funding

This project was supported by Researchers Supporting Project number (RSPD2023R712), King Saud University, Riyadh, Saudi Arabia.

Competing interests

The authors declare no competing interests.

Availability of data and materials

All data generated and analysed are included in the submitted manuscript and supplementary materials.

Acknowledgement

The authors thank DST- FIST (New Delhi, India) and The Management of PSG College of Arts & Science, Coimbatore, for conducting this research.

Financial interests

The authors have no relevant financial or non-financial interests to disclose.

References

1. J. Cardoso, D. G. Nakayama, E. Sousa, and E. Pinto. (2020). Marine-Derived Compounds and Prospects for Their Antifungal Application. *Molecules,* 25(24), 5856. https://doi.org/10.3390/molecules25245856
2. Šimat V, Elabed N, Kulawik P, Ceylan Z, Jamroz E, Yazgan H, Čagalj M, Regenstein JM, Özogul F. (2020). Recent Advances in Marine-Based Nutraceuticals and Their Health Benefits. *Marine Drugs,* 18(12): 627. https://doi.org/10.3390/md18120627
3. J. Suresh, G. Pradheesh, V. Alexramani, M. Sundrarajan, and S. I. Hong. (2018). Green synthesis and characterization of zinc oxide nanoparticle using insulin plant (Costus pictus D. Don) and investigation of its antimicrobial as well as anticancer activities. *Advances in Natural Sciences: Nanoscience and Nanotechnology*, 9(1), 15008. https://doi.org/10.1088/2043-6254/aaa6f1
4. S. Ahmed, M. Ahmad, B. L. Swami, and S. Ikram. (2016). A review on plants extract mediated synthesis of silver nanoparticles for antimicrobial applications: A green expertise. *Journal of Advanced Research*, 7(1), 17–28.https://doi.org/10.1016/j.jare.2015.02.007
5. D. Uvarajan and B. Durairaj. (2022) Antimicrobial Potential of Zinc Oxide Nanoparticles from Marine Macroalgae. *Int J Res Appl Sci Eng Technol*, 10(3), 676–679. https://doi.org/10.22214/ijraset.2022.40608
6. Motshakeri, M., Ebrahimi, M., Goh, Y. M., Matanjun, P., and Mohamed, S. (2013). *Sargassum polycystum* reduces hyperglycaemia, dyslipidaemia and oxidative stress via increasing insulin sensitivity in a rat model of type 2 diabetes. *Journal of the science of food and agriculture*, 93(7), 1772–1778. https://doi.org/10.1002/jsfa.5971

7. Motshakeri, M., Ebrahimi, M., Goh, Y. M., Othman, H. H., Hair-Bejo, M., and Mohamed, S. (2014). Effects of Brown Seaweed (*Sargassum polycystum*) Extracts on Kidney, Liver, and Pancreas of Type 2 Diabetic Rat Model. *Evidence-based complementary and alternative medicine*, 379407. https://doi.org/10.1155/2014/379407
8. E. Haque and A. C. Ward. (2018). Zebrafish as a model to evaluate nanoparticle toxicity. *Nanomaterials*, 8(7), 561. https://doi.org/10.3390/nano8070561
9. C. de Souza Anselmo, V. F. Sardela, V. P. de Sousa, and H. M. G. Pereira. (2018). Zebrafish (Danio rerio): A valuable tool for predicting the metabolism of xenobiotics in humans?. *Comparative Biochemistry and Physiology Part - C: Toxicology and Pharmacology*, 212, 34–46. https://doi.org/10.1016/j.cbpc.2018.06.005
10. Kteeba, S. M., El-Adawi, H. I., El-Rayis, O. A., El-Ghobashy, A. E., Schuld, J. L., Svoboda, K. R., and Guo, L. (2017). Zinc oxide nanoparticle toxicity in embryonic zebrafish: Mitigation with different natural organic matter. *Environmental pollution*, 230, 1125–1140. https://doi.org/10.1016/j.envpol.2017.07.042
11. J. S. van Dyk and B. Pletschke. (2011). Review on the use of enzymes for the detection of organochlorine, organophosphate and carbamate pesticides in the environment. *Chemosphere*, 82(3), 291–307. https://doi.org/10.1016/j.chemosphere.2010.10.033
12. Marcellin-Gros, R., Piganeau, G., and Stien, D. (2020). Metabolomic Insights into Marine Phytoplankton Diversity. *Marine drugs*, 18(2), 78. https://doi.org/10.3390/md18020078
13. Ali, O., Ramsubhag, A., and Jayaraman, J. (2021). Biostimulant Properties of Seaweed Extracts in Plants: Implications towards Sustainable Crop Production. *Plants*, 10(3), 531. https://doi.org/10.3390/plants10030531
14. Xu M, Zhang Q, Lin X, Shang Y, Cui X, Guo L, Huang Y, Wu M, Song K. (2023). Potential Effects of Metal Oxides on Agricultural Production of Rice: A Mini Review. *Plants*,12(4): 778. https://doi.org/10.3390/plants12040778
15. Lahiri, D., Ray, R. R., Sarkar, T., Upadhye, V. J., Ghosh, S., Pandit, S., Pati, S., Edinur, H. A., Abdul Kari, Z., Nag, M., and Ahmad Mohd Zain, M. R. (2022). Anti-biofilm efficacy of green-synthesized ZnO nanoparticles on oral biofilm: In vitro and in silico study. *Frontiers in microbiology*, 13, 939390. https://doi.org/10.3389/fmicb.2022.939390
16. M. Hassellöv, J. W. Readman, J. F. Ranville, and K. Tiede. (2008). Nanoparticle analysis and characterization methodologies in environmental risk assessment of engineered nanoparticles. *Ecotoxicology*, 17(5), 344–361. https://doi.org/10.1007/s10646-008-0225-x
17. M. S. Geetha, H. Nagabhushana, and H. N. Shivananjaiah. (2016). Green mediated synthesis and characterization of ZnO nanoparticles using Euphorbia Jatropa latex as reducing agent. *Journal of Science: Advanced Materials and Devices*, 1(3), 301–310. https://doi.org/10.1016/j.jsamd.2016.06.015
18. Alamdari S, SasaniGhamsari M, Lee C, Han W, Park H-H, Tafreshi MJ, Afarideh H, Ara MHM. (2020). Preparation and Characterization of Zinc Oxide Nanoparticles Using Leaf Extract of Sambucus

ebulus. *Applied Sciences*, 10(10), 3620. https://doi.org/10.3390/app10103620

19. Pallavi S.S., Hassan Ahmed Rudayni, Asmatanzeem Bepari, Shaik Kalimulla Niazi, Sreenivasa Nayaka. (2022). Green synthesis of Silver nanoparticles using Streptomyces hirsutus strain SNPGA-8 and their characterization, antimicrobial activity, and anticancer activity against human lung carcinoma cell line A549. *Saudi Journal of Biological Sciences*, 29(1), 228-238. https://doi.org/10.1016/j.sjbs.2021.08.084
20. C Kimmel, C. B., Ballard, W. W., Kimmel, S. R., Ullmann, B., and Schilling, T. F. (1995). Stages of embryonic development of the zebrafish. *Developmental dynamics : an official publication of the American Association of Anatomists*, 203(3), 253–310. https://doi.org/10.1002/aja.1002030302
21. N. A. Thirumurthi, A. Raghunath, S. Balasubramanian, and E. Perumal. (2022). Evaluation of Maghemite Nanoparticles–Induced Developmental Toxicity and Oxidative Stress in Zebrafish Embryos/Larvae. *Biol Trace Elem Res*, 200(5), 2349–2364. https://doi.org/10.1007/s12011-021-02830-y
22. Finney, D.J. (1971). Probit Analysis. *Cambridge University Press*, 333. https://doi.org/10.1002/jps.2600600940
23. B. Fraysse, R. Mons, and J. Garric. (2006). Development of a zebrafish 4-day embryo-larval bioassay to assess toxicity of chemicals. *Ecotoxicol Environ Saf*, 63(2), 253–267. https://doi.org/10.1016/j.ecoenv.2004.10.015
24. O. H. Lowry, N. J. Rosebrough, A. L. farr, and R. J. Randall. (1951). Protein measurement with the Folin phenol reagent. *J Biol Chem*, 193(1), 265–275.
25. Ellman, G. L., courtney, K. D., Andres, V., Jr, and Feather-stone, R. M. (1961). A new and rapid colorimetric determination of acetylcholinesterase activity. *Biochemical pharmacology*, 7, 88–95. https://doi.org/10.1016/0006-2952(61)90145-9
26. Bonting, S. L., Simon, K. A., and Hawkins, N. M. (1961). Studies on sodium-potassium-activated adenosine triphosphatase. I. Quantitative distribution in several tissues of the cat. *Archives of biochemistry and biophysics*, 95, 416–423. https://doi.org/10.1016/0003-9861(61)90170-9
27. C. H. Fiske and Y. Subbarow. (1925). The colorimetric determination of phosphorus. *Journal of Biological Chemistry*, 66(2), 375–400. https://doi.org/10.1042/bj0260292
28. Beauchamp, C., and Fridovich, I. (1971). Superoxide dismutase: improved assays and an assay applicable to acrylamide gels. *Analytical biochemistry*, 44(1), 276–287. https://doi.org/10.1016/0003-2697(71)90370-8
29. Devasagayam, T. P., and Tarachand, U. (1987). Decreased lipid peroxidation in the rat kidney during gestation. *Biochemical and biophysical research communications*, 145(1), 134–138. https://doi.org/10.1016/0006-291x(87)91297-6
30. Levine, R. L., Garland, D., Oliver, C. N., Amici, A., Climent, I., Lenz, A. G., Ahn, B. W., Shaltiel, S., and Stadtman, E. R. (1990). Determination of carbonyl content in oxidatively modified proteins. *Methods in enzymology*, 186, 464–478. https://doi.org/10.1016/0076-6879(90)86141-h

31. Green, L. C., Wagner, D. A., Glogowski, J., Skipper, P. L., Wishnok, J. S., and Tannenbaum, S. R. (1982). Analysis of nitrate, nitrite, and [15N]nitrate in biological fluids. *Analytical biochemistry*, 126(1), 131–138. https://doi.org/10.1016/0003-2697(82)90118-x
32. Hugo Abei. (1984). Catalsae in vitro, *Methods in Enzymology*, 105, 121-126. https://doi.org/10.1016/S0076-6879(84)05016-3
33. Rotruck, J. T., Pope, A. L., Ganther, H. E., Swanson, A. B., Hafeman, D. G., and Hoekstra, W. G. (1973). Selenium: biochemical role as a component of glutathione peroxidase. *Science*, 179(4073), 588–590. https://doi.org/10.1126/science.179.4073.588
34. Habig, W. H., and Jakoby, W. B. (1981). Assays for differentiation of glutathione S-transferases. *Methods in enzymology*, 77, 398–405. https://doi.org/10.1016/s0076-6879(81)77053-8
35. Aihua Gu, Xiangguo Shi, Chen Yuan, Guixiang Ji, Yong Zhou, Yan Long, Ling Song, Shoulin Wang, Xinru Wang. (2010). Exposure to fenvalerate causes brain impairment during zebrafish development. *Toxicology Letters*, 197(3), 188-192. https://doi.org/10.1016/j.toxlet.2010.05.021
36. G. Vale, K. Mehennaoui, S. Cambier, G. Libralato, S. Jomini, and R. F. Domingos, (2016). Manufactured nanoparticles in the aquatic environment-biochemical responses on freshwater organisms: A critical overview. *Aquatic Toxicology*, 170, 162–174. https://doi.org/10.1016/j.aquatox.2015.11.019
37. Deenathayalan and D. Brindha. (2022). Antioxidant potential of biosynthesized zinc oxide nanoparticles from Sargassum polycystum aqueous extract. *Research Journal of Biotechnology*, 17(7), 10-15. https://doi.org/10.25303/1707rjbt01015
38. Selvakumar Sakthivel, Anand Raj Dhanapal, Lilly Pushpa Paulraj, Annadurai Gurusamy, Baskar Venkidasamy, Muthu Thiruvengadam, Rajakumar Govindasamy, Mohammad Ali Shariati, Abdelhakim Bouyahya, Gokhan Zengin, Mohammad Mehedi Hasan, Pavel Burkov. (2022). Antibacterial activity of seed aqueous extract of Citrus limon (L.) mediated synthesis ZnO NPs: An impact on Zebrafish (Danio rerio) caudal fin development. *Heliyon*, 8(9), 10406. https://doi.org/10.1016/j.heliyon.2022.e10406
39. J. S. Choi, R. O. Kim, S. Yoon, and W. K. Kim. (2016). Developmental Toxicity of Zinc Oxide Nanoparticles to Zebrafish (Danio rerio): A transcriptomic analysis. *PLoS One*, 11(8), 160763. https://doi.org/10.1371/journal.pone.0160763
40. G. M. T. de Oliveira, E. M. N. de Oliveira, T. C. B. Pereira, R. M. Papaléo, and M. R. Bogo, (2017). Implications of exposure to dextran-coated and uncoated iron oxide nanoparticles to developmental toxicity in zebrafish. *J Nanopart Res*, 19, 389. https://doi.org/10.1007/s11051-017-4074-5
41. D M. Rawson,T. Zhang, D. Kalicharan, W L. Jongebloed. (2001). Field emission scanning electron microscopy and transmission electron microscopy studies of the chorion, plasma membrane and syncytial layers of the gastrula-stage embryo of the zebrafish Brachydanio rerio: a consideration of the structural and functional relationships with respect to cryoprotectant penetration. *Aquaculture research*, 31(3), 325-336. https://doi.org/10.1046/j.1365-2109.2000.00401.x

42. P. v. Asharani, Y. Lian Wu, Z. Gong, and S. Valiyaveettil. (2008). Toxicity of silver nanoparticles in zebrafish models. *Nanotechnology*, 19(25). https://doi.org/10.1088/0957-4484/19/25/255102
43. Rubbo, H., Parthasarathy, S., Barnes, S., Kirk, M., Kalyanaraman, B., and Freeman, B. A. (1995). Nitric oxide inhibition of lipoxygenase-dependent liposome and low-density lipoprotein oxidation: termination of radical chain propagation reactions and formation of nitrogen-containing oxidized lipid derivatives. *Archives of biochemistry and biophysics*, 324(1), 15–25. https://doi.org/10.1006/abbi.1995.9935
44. Pott, A., Bock, S., Berger, I. M., Frese, K., Dahme, T., Keßler, M., Rinné, S., Decher, N., Just, S., and Rottbauer, W. (2018). Mutation of the Na+/K+-ATPase Atp1a1a.1 causes QT interval prolongation and bradycardia in zebrafish. *Journal of molecular and cellular cardiology*, 120, 42–52. https://doi.org/10.1016/j.yjmcc.2018.05.005
45. Bai, W., Zhang, Z., Tian, W. (2010). Toxicity of zinc oxide nanoparticles to zebrafish embryo: a physicochemical study of toxicity mechanism. *J Nanopart Res,* 12, 1645–1654 (2010). https://doi.org/10.1007/s11051-009-9740-9
46. Rajaduraipandian Subramanian, Gabrial Kathirason Sabeena, M. Ponnanikajamideen S. Rajeshkumar, G. Annadurai, Gandhimathi Sivasubramanian. (2022). Synthesis of Green Zinc Oxide Nanoparticles Mediated by Syzygiumcumini Induced Developmental Deformation in Embryo Toxicity of (Daniorerio) Zebrafish, *Iran J. Chem. Chem. Eng,* 41(12), 3895-3904. https://doi.org/10.30492/IJCCE.2022.543395.5026
47. Soreq, H., and Seidman, S. (2001). Acetylcholinesterase–new roles for an old actor. Nature reviews. *Neuroscience*, 2(4), 294–302. https://doi.org/10.1038/35067589
48. Suganya, D., Ramakritinan, C.M. and Rajan, M.R. (2018). Adverse Effects of Genotoxicity, Bioaccumulation and Ionoregulatory Modulation of Two Differently Synthesized Iron Oxide Nanoparticles on Zebrafish (Danio rerio). *J Inorg OrganometPolym*, 28, 2603–2611. https://doi.org/10.1007/s10904-018-0935-3
49. Lian-Jiu Su, Jia-Hao Zhang, Hernando Gomez, Raghavan Murugan, Xing Hong, Dongxue Xu, Fan Jiang, Zhi-Yong Peng. (2019). Reactive Oxygen Species-Induced Lipid Peroxidation in Apoptosis, Autophagy, and Ferroptosis. *Oxidative Medicine and Cellular Longevity*, 13. https://doi.org/10.1155/2019/5080843
50. D. T. Jayaram, S. Runa, M. L. Kemp, and C. K. Payne. (2017). Nanoparticle-induced oxidation of corona proteins initiates an oxidative stress response in cells. *Nanoscale*, 9(22), 7595–7601. https://doi.org/10.1039/c6nr09500c
51. Vanaja, P., and Ekambaram, P. (2004). Demonstrating the dose- and time-related effects of 7-nitroindazole on picrotoxin-induced convulsions, memory formation, brain nitric oxide synthase activity, and nitric oxide concentration in rats. *Pharmacology, biochemistry, and behavior*, 77(1), 1–8. https://doi.org/10.1016/j.pbb.2003.08.020
52. Zhu, M. T., Wang, Y., Feng, W. Y., Wang, B., Wang, M., Ouyang, H., and Chai, Z. F. (2010). Oxidative stress and apoptosis induced by iron oxide nanoparticles in cultured human umbilical endothelial

cells. *Journal of nanoscience and nanotechnology*, 10(12), 8584–8590. https://doi.org/10.1166/jnn.2010.2488

53. R. Mani, S. Balasubramanian, A. Raghunath, and E. Perumal. (2020). Chronic exposure to copper oxide nanoparticles causes muscle toxicity in adult zebrafish. *Environ Sci Pollut Res,* 27, 27358–27369. https://doi.org/10.1007/s11356-019-06095-w
54. AnvariFar, H., Amirkolaie, A. K., Jalali, A. M., Miandare, H. K., Sayed, A. H., Üçüncü, S. İ., Ouraji, H., Ceci, M., and Romano, N. (2018). Environmental pollution and toxic substances: Cellular apoptosis as a key parameter in a sensible model like fish. *Aquatic toxicology*, 204, 144–159. https://doi.org/10.1016/j.aquatox.2018.09.010
55. Ge Y, Yuan W, Jia W, Guan Z, Huang T, Zhang Y, et al. (2023). Apoptotic mechanism of propofol-induced developmental toxicity in zebrafish embryos.*PLoS ONE,* 18(5), e0286391. https://doi.org/10.1371/journal.pone.0286391
56. Nagarajan, S., and Arumugam Kuppusamy, K. (2013). Extracellular synthesis of zinc oxide nanoparticle using seaweeds of gulf of Mannar, India. *Journal of nanobiotechnology*, 11, 39. https://doi.org/10.1186/1477-3155-11-39
57. Sharma, V., Anderson, D., and Dhawan, A. (2012). Zinc oxide nanoparticles induce oxidative DNA damage and ROS-triggered mitochondria mediated apoptosis in human liver cells (HepG2). *Apoptosis : an international journal on programmed cell death*, 17(8), 852–870. https://doi.org/10.1007/s10495-012-0705-6

Figures

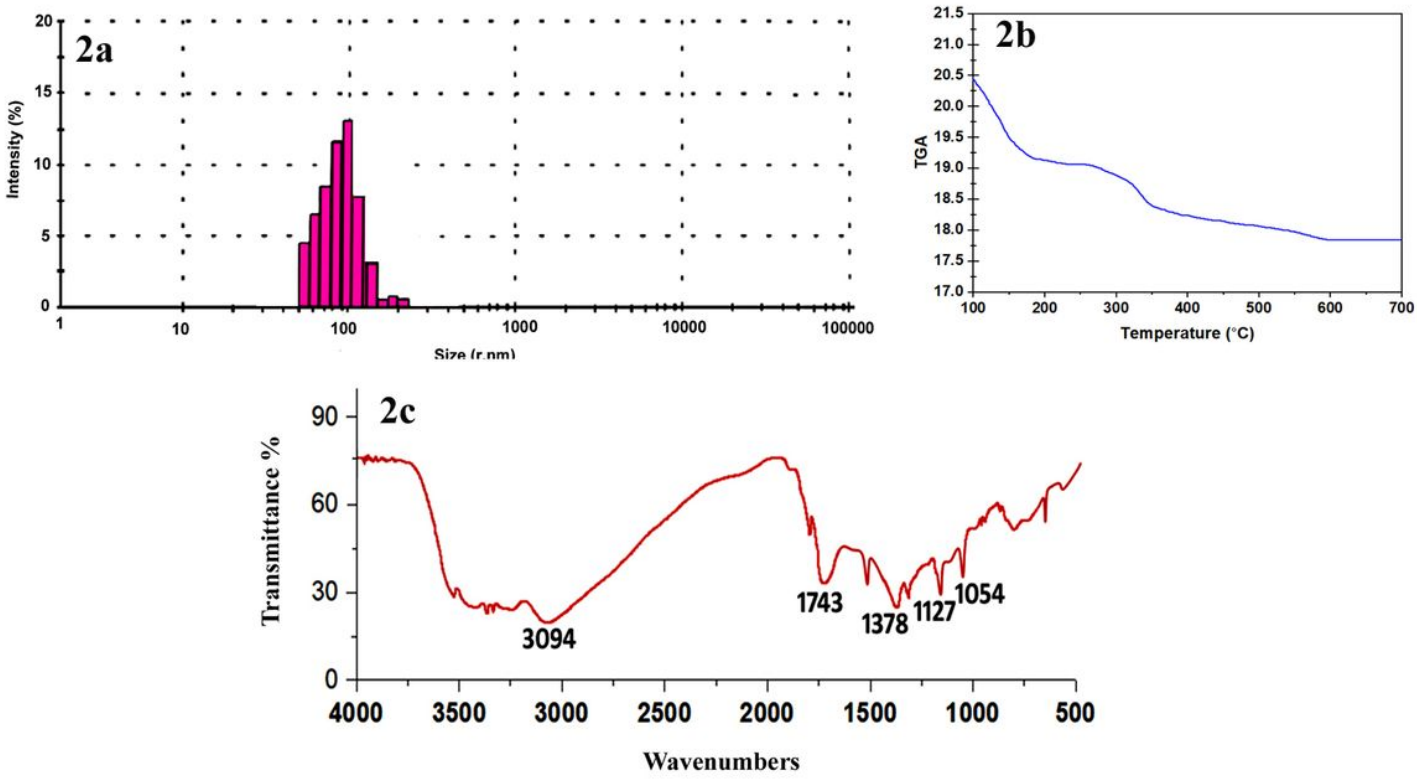

Figure 1

(a) DLS **(b)** TGA **(c)** FT- IR analysis of *S. Polycystum* mediated ZnONP's

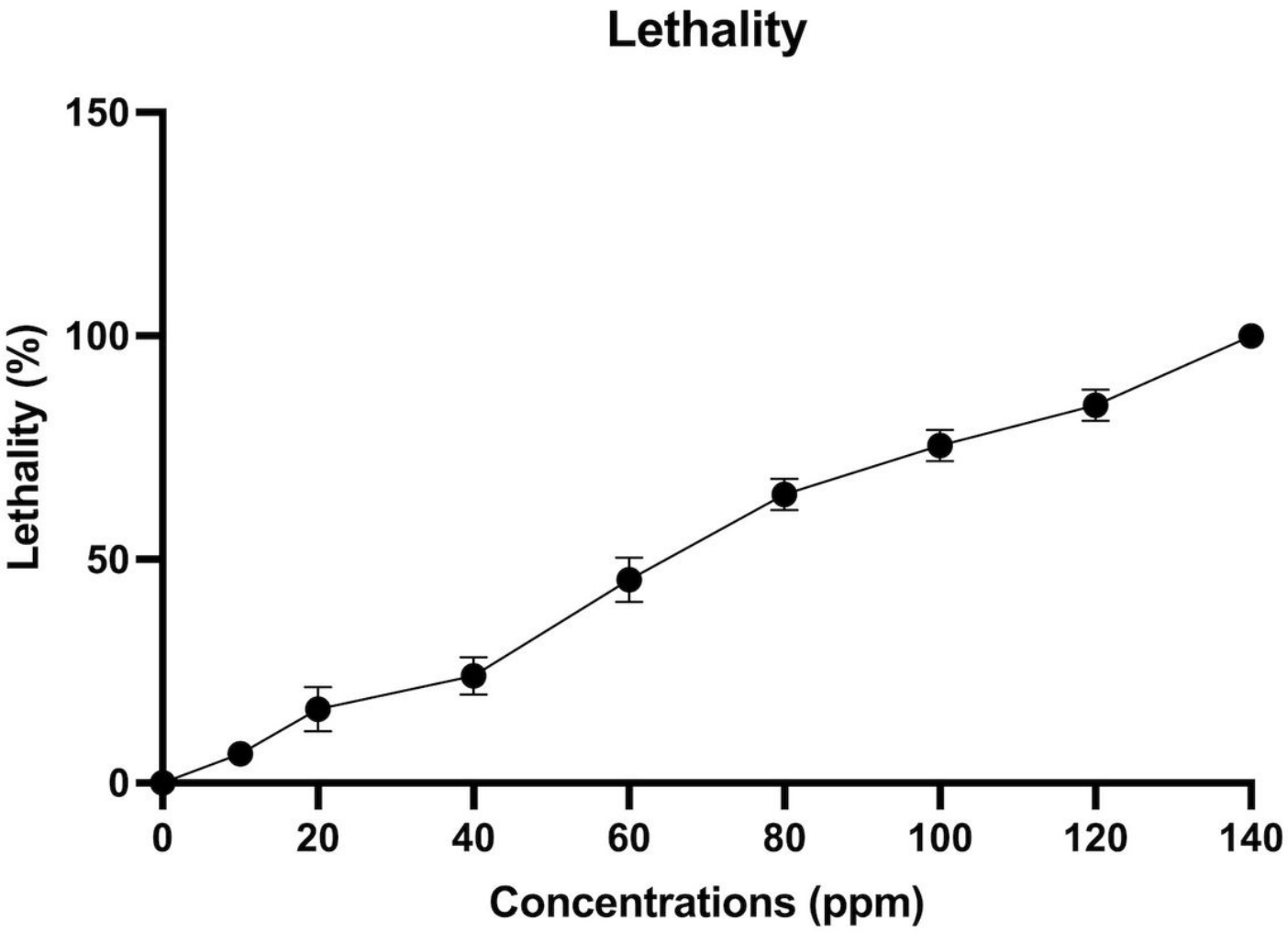

Figure 2

Lethality assay for the assessment of LC_{50} in ZnO NPs exposed zebrafish larvae at 96 hpf. Values are represented as mean± SD of three independent experiments

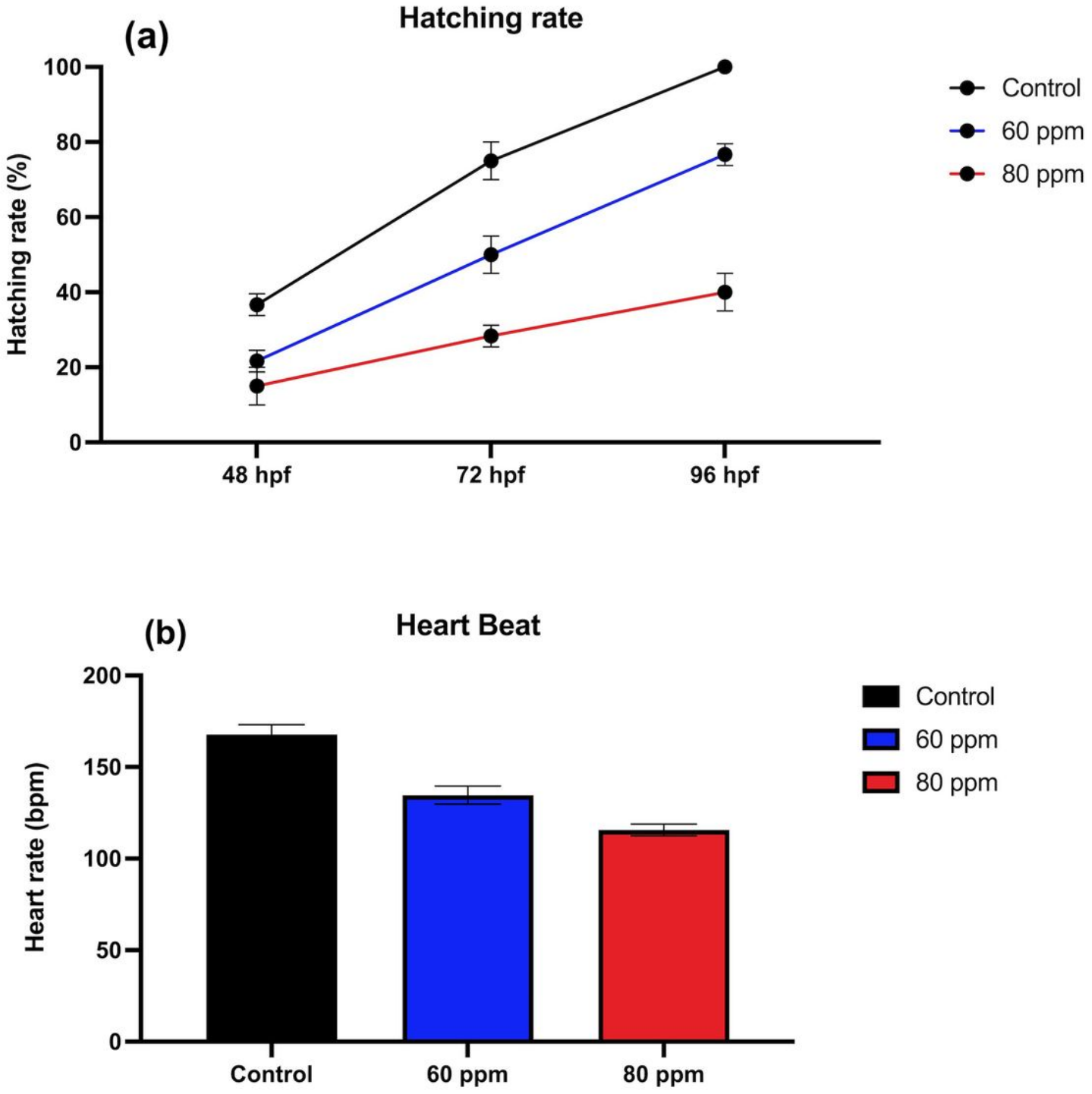

Figure 3

(**a**) Hatching rate and (**b**) heartbeat rate of control and treated groups. Values are represented as mean±SD of three independent experiments.

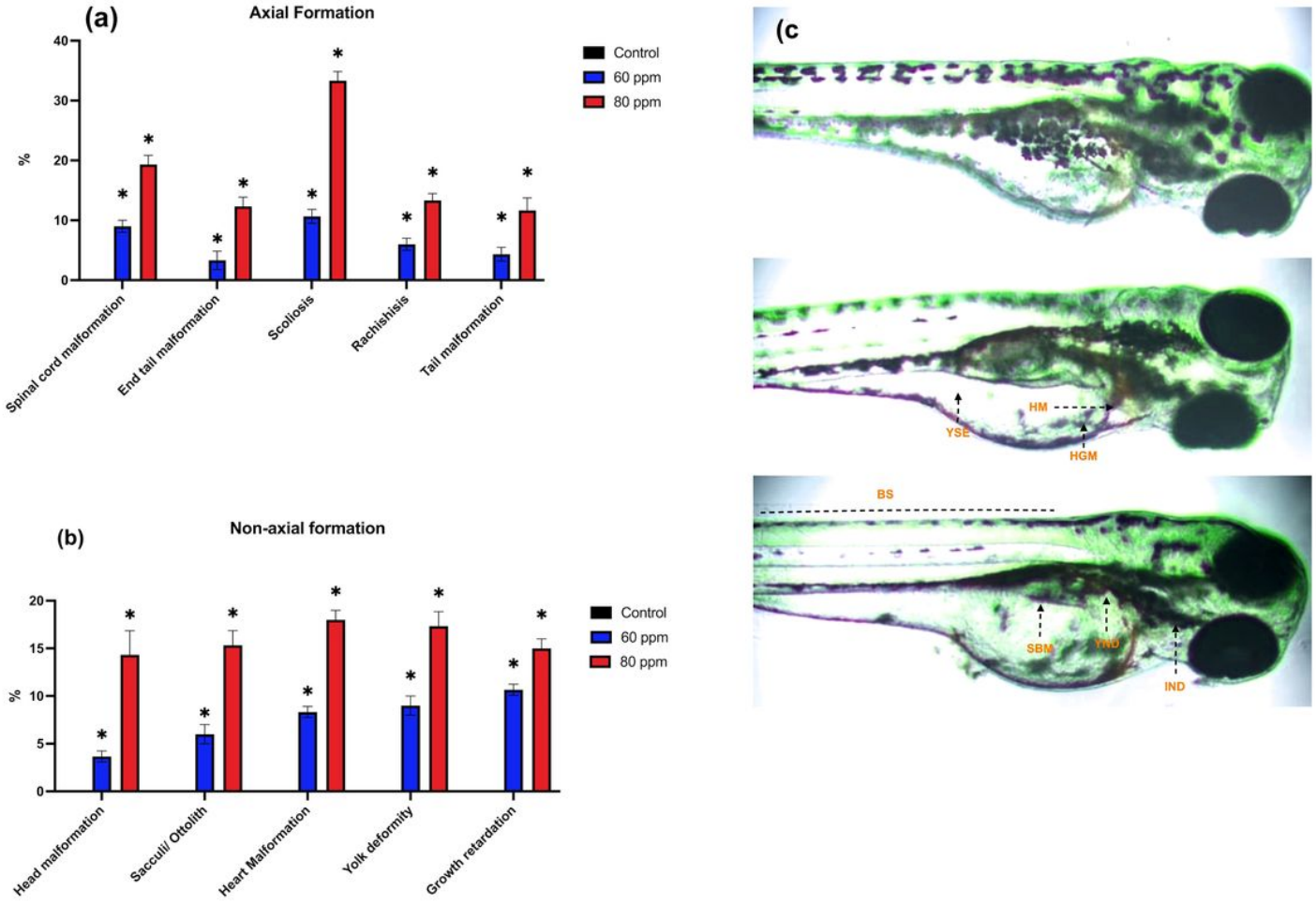

Figure 4

(**a**) Axial malformations (**b**) non-axial malformations, and (**c**) microscopic representative images of control and treated larvae at 96 hpf. Values are represented as mean± SD of three independent experiments. *p<0.05, compared with control (one-way ANOVA followed by Tukey's multiple comparison test)

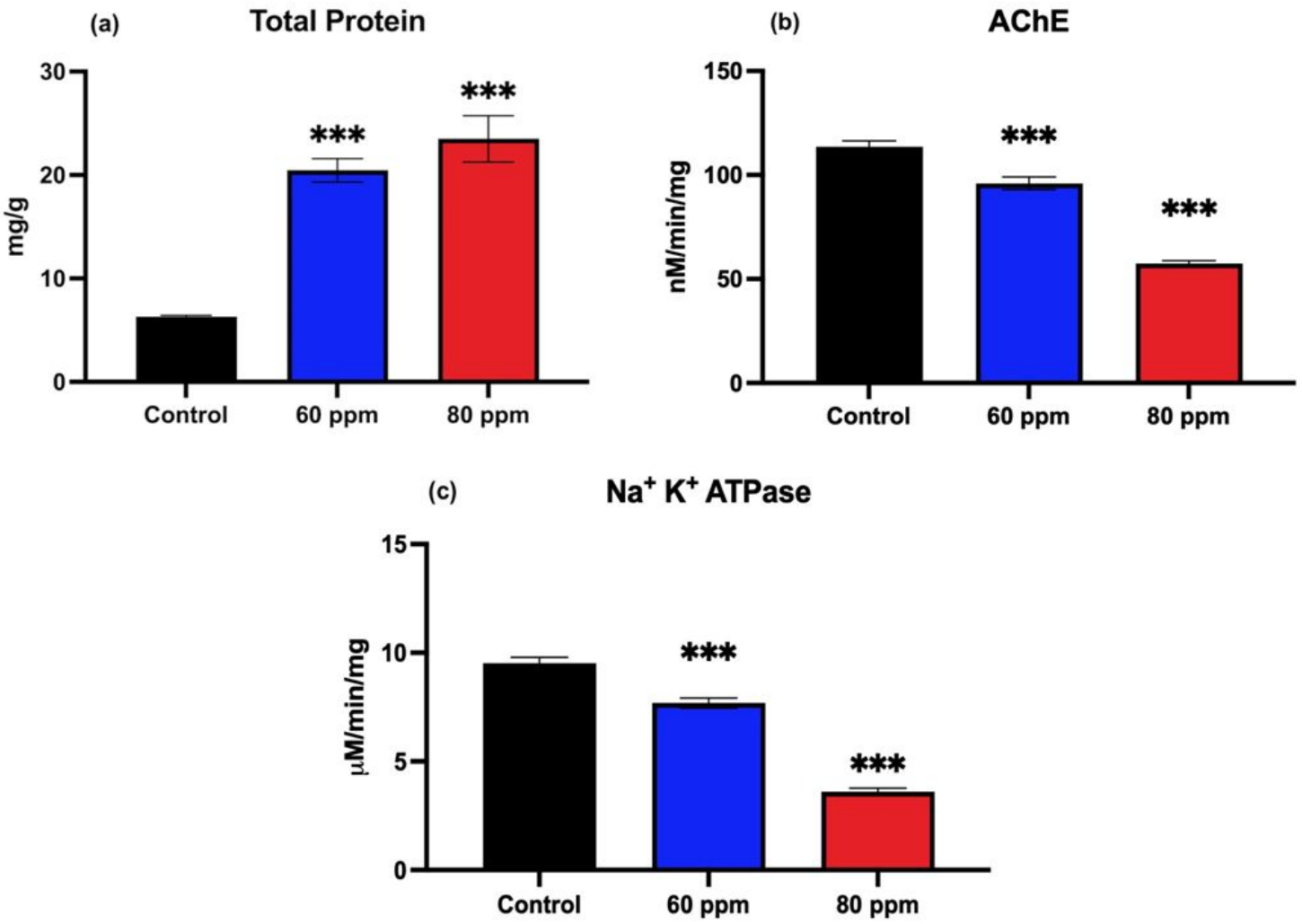

Figure 5

Alterations in the biochemical markers of control and treated larvae. (**a**) Total protein content (**b**) AChE, and (**c**) Na+ K+ ATPase. Values are represented as mean± SD of three independent experiments. ***p<0.001, compared with control (one-way ANOVA followed by Tukey's multiple comparison test)

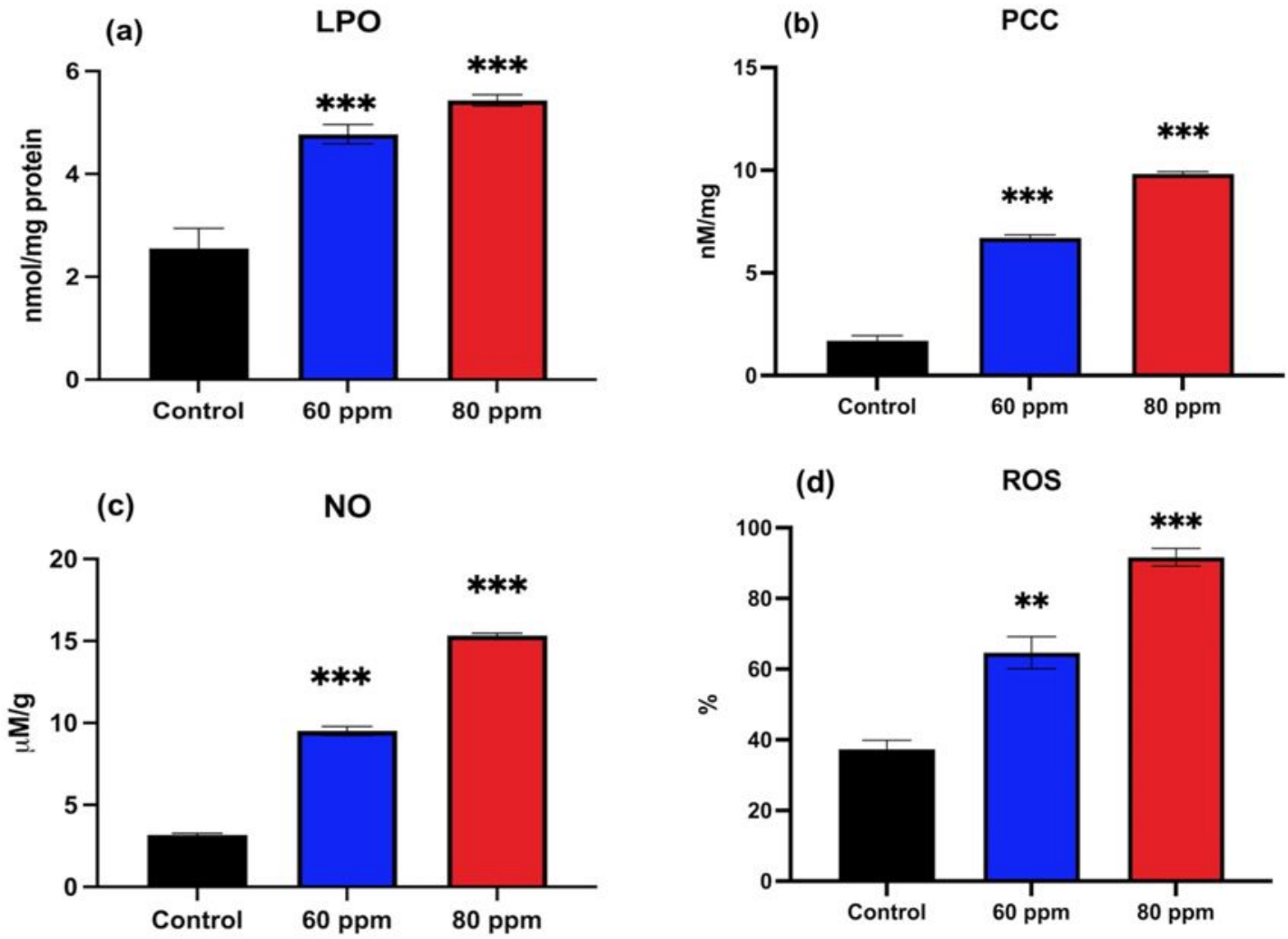

Figure 6

Alterations in the oxidant levels of control and treated larvae. (**a**) LPO (**b**) PCC (**c**) NO and (**d**) ROS. Values are represented as mean± SD of three independent experiments. **p<0.01, ***p<0.001 compared with control (one-way ANOVA followed by Tukey's multiple comparison test)

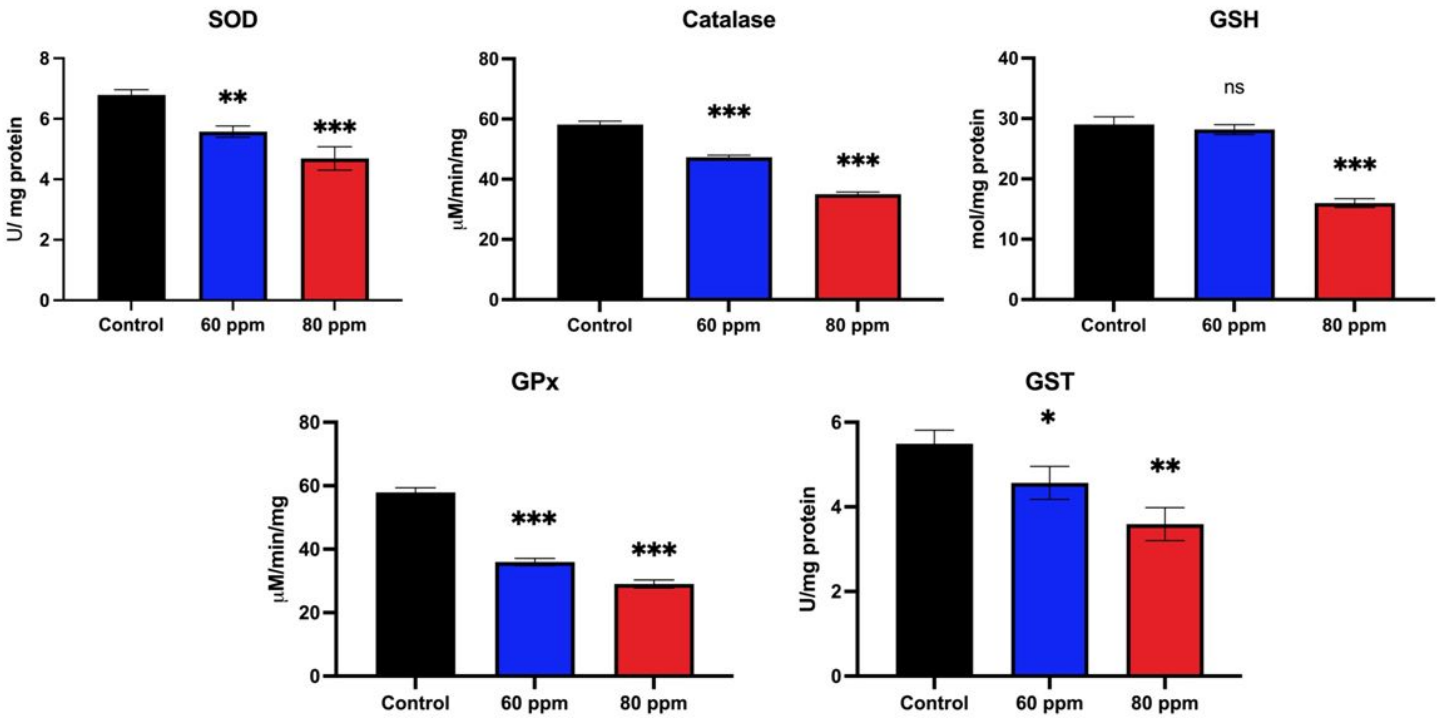

Figure 7

Alterations in the antioxidant levels of control and treated larvae. (**a**) SOD (**b**) CAT (**c**) GPx and (**d**) GST. Values are represented as mean± SD of three independent experiments. *p<0.05, **p<0.01, ***p<0.001, compared with control (one-way ANOVA followed by Tukey's multiple comparison test)

Supplementary Files

This is a list of supplementary files associated with this preprint. Click to download.

- Supplementryfile.docx